Solid-State NMR Study of the Role of H and Na in AB-Type Carbonate Hydroxylapatite

Harris E. Mason,*[,†,‡] Andrew Kozlowski,[†,§] and Brian L. Phillips[†,‡]

Center for Environmental Molecular Science and Department of Geosciences, State University of New York, Stony Brook, New York, 11794-2100, and Department of Chemistry, St. Lawrence University, Canton, New York 13617

Received June 20, 2007. Revised Manuscript Received October 10, 2007

Solid-state nuclear magnetic resonance (NMR) techniques, combined with Fourier transform infrared (FT-IR) spectroscopy, were used to study synthetic AB-type carbonate hydroxylapatite (CHAp). $^{13}C\{^{1}H\}$ heteronuclear correlation (HetCor) experiments indicate that the two carbonate environments represented by the peaks at $\delta_C = 169.8$ and 170.8 ppm are associated with three H environments with one environment represented by a peak centered about $\delta_H = 0.0$ ppm and two additional peaks located at 1.3 and 5.5 ppm. The peaks near $\delta_H = 0.0$ ppm correspond to hydroxyl environments within the channels of the CHAp, whereas those at 1.3 and 5.5 exhibit spectral characteristics consistent with bicarbonate ions that donate moderate to weak hydrogen bonds. Possible methods by which bicarbonate incorporation can be accommodated by the apatite structure are discussed. The Na/carbonate ratio and ^{23}Na NMR spectroscopy indicate that Na plays an important role in the carbonate incorporation in these materials.

Introduction

Carbonate-containing hydroxylapatite (CHAp) has been the subject of numerous studies spanning a broad range of disciplines. This material is of interest to the medical and dental fields because the inorganic component of teeth and bones is best described by nanometer-sized particles of hydroxylapatite containing significant concentrations of carbonate impurity (~8 wt%).[1] CHAp has also been studied with relevance to the fields of both material sciences and geochemistry because of the changes in reactivity and solubility of hydroxylapatite when carbonate is present as a trace anion.[2] Bone apatite is commonly used in permeable reactive barriers and has been shown to effectively sequester heavy metal cations and radionuclides.[3,4] It is, therefore, important to understand how carbonate is incorporated in apatite and what accommodations must be made in order for it to successfully integrate within the apatite structure.

Previous studies have shown that two principal modes of carbonate substitution can exist within the apatite structure. The first substitution mechanism (A-site substitution) involves the replacement of channel site hydroxyl ions with carbonate. The second mechanism (B-site substitution) corresponds to the carbonate replacing a phosphate group.[2,5] Although pure phases containing only A-type substitution or B-type substitution have been successfully synthesized,[6,7] CHAp can also be produced, which contains substitution in both the A and B sites denoted as AB-type CHAp.[8,9] All CHAp phases have been synthesized in aqueous systems;[1,5,7,10] however, many studies produce CHAp under high-temperature, high-pressure conditions in order to produce crystals suitable for X-ray and neutron diffraction studies.[6,9,11–13] Recently, Fleet and Liu[9] suggested that in sodium-bearing AB-type CHAp, the A and B carbonate substitutions were coupled through substitutions in neighboring A and B sites. Structure refinements of XRD data gave O···O distances between the A-type carbonate group and the phosphate tetrahedron that were too short for simultaneous occupancy, which was interpreted to indicate B-type substitution in the adjacent PO_4 site.

The A- and B-type carbonate substitutions in CHAp can be distinguished by Fourier transform infrared (FT-IR) spectroscopy. These substitutions give a distinct splitting in the υ_3 carbonate mode, where A- and B-type yield distinct peaks at 880 and 875 cm^{-1}, respectively.[5,11,13] Additionally, differences in the υ_2 region from 1545 to 1410 cm^{-1} have been used to differentiate these substitution sites.[11] Recently, however, Fleet and Liu[9] have indicated that the presence of

* Corresponding author. Phone: (631) 632-1454. Fax: (631) 632-6840. E-mail: hmason@ic.sunysb.edu.
† Center for Environmental Molecular Science, State University of New York.
‡ Department of Geosciences, State University of New York.
§ St. Lawrence University.

(1) Barralet, J.; Best, S.; Bonfield, W. *J. Biomed. Mater. Res.* **1998**, *41*, 79.
(2) Elliott, J. C. *Rev. Mineral. Geochem.* **2002**, *48*, 427.
(3) Conca, J. L.; Wright, J. *Appl. Geochem.* **2006**, *21*, 1288.
(4) Wright, J.; Rice, K. R.; Murphy, B.; Conca, J. *Sustainable Range Management*; Battelle Press: Columbus, OH, 2004.
(5) Nelson, D. G. A.; Featherstone, J. D. B. *Calcified Tissue Int.* **1982**, *34*, S69.
(6) Fleet, M. E.; Liu, X. Y. *J. Solid State Chem.* **2003**, *174*, 412.
(7) Beshah, K.; Rey, C.; Glimcher, M. J.; Schimizu, M.; Griffin, R. G. *J. Solid State Chem.* **1990**, *84*, 71.
(8) Fleet, M. E.; Liu, X. Y. *J. Solid State Chem.* **2004**, *177*, 3174.
(9) Fleet, M. E.; Liu, X. *Biomaterials* **2007**, *28*, 916.
(10) Wilson, R. M.; Elliott, J. C.; Dowker, S. E. P.; Smith, R. I. *Biomaterials* **2004**, *25*, 2205.
(11) Fleet, M. E.; Liu, X. Y.; King, P. L. *Am. Mineral.* **2004**, *89*, 1422.
(12) Wilson, R. M.; Dowker, S. E. P.; Elliott, J. C. *Biomaterials* **2006**, *27*, 4682.
(13) Suetsugu, Y.; Shimoya, I.; Tanaka, J. *J. Am. Ceram. Soc.* **1998**, *81*, 746.

10.1021/cm0716598 CCC: $40.75
Published on Web 12/05/2007

sodium significantly changes the shape of the υ_2 region in AB-type CHAp compared to that of sodium-free AB-type CHAp.

Solid-state nuclear magnetic resonance (NMR) has also been employed in these systems to show the difference between the A and B sites in the apatites.[7,12] Beshah et al.[7] studied the system using $^{13}C\{^1H\}$ cross-polarization magic angle spinning (CP/MAS) NMR and showed that A-type CHAp gives a well-defined, narrow peak at about $\delta_C = 166.5$ ppm, B-type CHAp gives a broad, asymmetric peak centered at about 170.2 ppm, and AB-type CHAp produces a complex line shape containing a peak at 168.2 ppm in addition to the two peaks at the same position for A- and B-type CHAp. Using dipolar suppression techniques and heat treatment, the authors attributed the complex line shape observed in the AB-type CHAp to a combination of A-type, B-type, and a disordered carbonate species in contact with water adsorbed onto the surface.

In this study, we have prepared synthetic samples of AB-type carbonate hydroxylapatites (CHAp) under aqueous conditions (90 °C) and have characterized the substitutions using Fourier transform infrared (FT-IR) spectroscopy, Raman spectroscopy, and a variety of one- and two-dimensional solid-state nuclear magnetic resonance (NMR) spectroscopic techniques. These data indicate that two carbonate sites exist within the CHAp that are coupled to distinct H environments. We also provide evidence for the incorporation of hydrogen carbonate species into the CHAp structure. These results show that H as well as Na play a role in accommodating carbonate in the apatite structure.

Experimental Section

Sample Synthesis. A series of samples of AB-type CHAp were synthesized using a method adapted from Nelson and Featherstone.[5] An initial CHAp (AK-2) was precipitated from aqueous solution by adding 40 mL of a solution containing 0.189 M ammonium hydrogen phosphate and 0.0589 M sodium bicarbonate at a rate of 0.55 mL/min to 40 mL of a continuously stirred 0.212 M calcium nitrate solution under a nitrogen atmosphere at 90 °C. The pH of the reaction was maintained between 8.5 and 9.5 by periodic manual additions of small amounts of 10 N NaOH. The precipitate was collected, centrifuged, rinsed in deionized water, and dried in an oven at 100 °C for 14 h. A portion of this sample was then placed in a PTFE-lined hydrothermal vessel with a solution containing 1 M sodium bicarbonate and heated to 200 °C under autogenous pressure for 2 days in an attempt to increase the crystallinity of the sample (AK-2H). This same method was used to prepare a partially dueterated sample (AK-2HD) from the AK-2H sample where the sodium bicarbonate solution in the hydrothermal vessel was prepared in 98% D_2O.

Additional samples of aqueous precipitated (AK-4) and hydrothermally treated (AK-5H) CHAp were prepared following the same methods as above but using solutions containing ^{13}C-enriched sodium bicarbonate. AK-4 was vacuumed filtered, washed with acetone, and allowed to dry in a 100 °C oven for 30 min. AK-5H was collected, centrifuged, washed with DI water and allowed to dry in a desiccator at room temperature for 18 h. Although collection methods differed for these samples, no major differences were observed in the XRD patterns of these samples from those that were otherwise prepared.

Analytical Methods. Elemental analyses for Na, Ca, and P were done using a Beckman Spectraspan SSUU direct current plasma emission spectrometer on portions of the AK-4 and AK-5H samples dissolved in a 23 mM HCl solution. Standards were prepared to mimic the compositions of the sample solutions to minimize matrix effects in the analysis. Carbonate content of the samples was estimated from correlations between Raman spectral features and carbonate content developed by Krajewski et al.[14]

X-ray powder diffraction (XRD) patterns were collected using a Scintag PADX powder X-ray diffractometer to verify the phase purity of all the synthetic samples, and in all cases, a single phase CHAp was produced. Fourier transform infrared (FT-IR) spectra were collected over a range of 650 to 4000 cm^{-1} on a Nicolet 670 FT-IR spectrometer in adsorption mode. Samples were ground in an agate mortar with spectroscopic grade KBr in an approximate 1:10 ratio of sample to KBr, and spectra were collected for 128 scans at a resolution of 1 cm^{-1}. Raman spectra were collected over a range of 200 to 3900 cm^{-1} on an InPhotonics RS-2000 Raman spectrometer at a resolution of 1 cm^{-1}.

Most NMR spectra were collected on a 400 MHz Varian Inova spectrometer at operating frequencies of 399.76, 161.82, and 100.57 MHz for ^1H, ^{31}P, and ^{13}C, respectively. ^1H single-pulse magic angle spinning (SP/MAS) NMR spectra were collected at a spinning rate of 15 kHz on a Chemagnetics probe configured for 4 mm (o.d.) rotors and modified to yield a very low ^1H background signal, which is insignificant compared to signal from the samples and was not subtracted from the spectra. $^{31}P\{^1H\}$ two-dimensional (2D) heteronuclear correlation (HetCor) and $^{13}C\{^1H\}$ 2D HetCor spectra were acquired with a Varian/Chemagnetics 3.2 mm T3 probe assembly at a 10 kHz spinning rate. For the $^{13}C\{^1H\}$ HetCor, we acquired a total of 64 hypercomplex points in $t1$ with a 100 μs increment, corresponding to a 10 kHz F1 spectral window, at contact times from 0.5 to 10.0 ms using a linear ramp of the ^1H field to optimize signal intensity. For the $^{31}P\{^1H\}$ HetCor spectra, a total of 128 hypercomplex points in $t1$ were collected with a 20 μs increment, corresponding to a 50 kHz F1 spectral window. All HetCor NMR data were processed with standard linear prediction methods to complete the signal in $t1$. ^1H spectra were referenced to tetramethylsilane (TMS) by setting the hydroxyl resonance in a standard reagent grade hydroxylapatite to $\delta_H = 0.2$ ppm.[15] ^{31}P spectra were referenced with respect to 85% H_3PO_4 using the same hydroxylapatite as an external reference set to $\delta_P = 2.65$ ppm (which had been measured previously by substitution). ^{13}C spectra were referenced with respect to TMS using adamantane as an external reference set to $\delta_C = 38.6$ ppm.[16] The ^1H dimension in the $^{13}C\{^1H\}$ HetCor was referenced with a $^{31}P\{^1H\}$ HetCor spectrum of hydroxylapatite obtained using the same F1 acquisition and processing parameters.

^{23}Na SP/MAS NMR, $^{23}Na\{^{31}P\}$ Rotational Echo Double Resonance (REDOR), and $^1H \rightarrow {}^{13}C\{^{31}P\}$ CP/REDOR spectra were collected on a 500 MHz Varian Infinity Plus spectrometer at operating frequencies of 499.78, 202.32, 132.17, and 125.69 MHz for ^1H, ^{31}P, ^{23}Na, and ^{13}C, respectively. ^{23}Na SP MAS NMR spectra were collected using a 1 μs pulse at a spinning rate of 18 kHz. $^{23}Na\{^{31}P\}$ REDOR spectra were collected at a spinning rate of 10 kHz using selective spin–echo pulses for ^{23}Na ($\pi = 15$ μs) and 8 μs recoupling pulses for ^{31}P. The $^1H \rightarrow {}^{13}C\{^{31}P\}$ CP/REDOR spectra were collected at a spinning rate of 5 kHz, using π-pulses of 12 μs on both the ^{13}C and ^{31}P channels and a 5 ms $^{13}C\{^1H\}$ CP preparation. ^{23}Na SP/MAS and multiple quantum (MQ) MAS NMR

(14) Krajewski, A.; Mazzocchi, M.; Buldini, P. L.; Ravaglioli, A.; Tinti, A.; Taddei, P.; Fagnano, C. *J. Mol. Struct.* **2005**, *744*, 221.
(15) Yesinowski, J. P.; Eckert, H. *J. Am. Chem. Soc.* **1987**, *109*, 6274.
(16) Earl, W. L.; Vanderhart, D. L. *J. Magn. Reson.* **1982**, *48*, 35.

spectra were collected on the 400 MHz spectrometer at 105.74 MHz and a spinning rate of 15 kHz. For the ^{23}Na MQMAS spectra, 2.9 μs excitation and 1.1 μs conversion pulses were used ($\nu_1 = 125$ kHz), followed by a selective 15 μs *z*-filtering pulse collecting a total of 128 hypercomplex points in $t1$ with a 20 μs increment.[17,18] ^{23}Na MQMAS NMR data were processed using standard shearing methods.[18] In all cases, ^{23}Na spectra were referenced with respect to an aqueous 1 M NaCl solution.

Results

Sample Composition. The chemical compositions of the ^{13}C-enriched AK-4 and AK-5H samples are similar to those of for sodium-bearing CHAp, which has been shown to be a reasonable analogue for human dental enamel.[9] These results give Na contents of 2.7 and 1.6 wt% and Ca:P molar ratios of 1.67 and 1.76 for AK-4 and AK-5H, respectively. Carbonate contents of the CHAp samples were estimated by the method proposed by Krajewski et al.[14] on the basis of a correlation of the intensity ratio between the Raman active υ_1 PO_4 peak at 962 cm^{-1} and the υ_1 CO_3 peak at 1072 cm^{-1} and elemental analyses for carbonate content. Using this correlation, we obtained values of approximately 5 and 7 wt% carbonate for the AK-4 and AK-5H samples, respectively. These values for AK-4 and AK-5H place the carbonate content of these samples within the range of that for natural biogenic apatites, such as bone apatite and dental enamel, which contain 3.5−8 wt% carbonate.[1,19] The molar ratios of Na:carbonate in these samples (1.4 and 0.6 for AK-4 and AK-5H respectively) suggest Na is important to the carbonate substitution mechanisms.

Vibrational Spectroscopy. The results for the vibrational spectroscopy for the samples AK-4, AK-5H, AK-2H and AK-2HD are summarized in Table 1. The Raman spectra (Figure SI-1, Supporting Information) of all samples contain peaks at 1086, 1050, 962, 608, 590, and 432 cm^{-1}which correspond to PO_4 modes.[5,14] A single peak at, 1072 cm^{-1}, was identified for CO_3 which corresponds to the υ_1 mode.[14] Hydroxyl modes were observed for the AK-2HD sample, for which a shifted OD peak was observed at 2636 cm^{-1}.

The FT-IR spectra (Figure 1) exhibit peaks characteristic of those previously described for carbonate groups present in the apatite structure.[5,6,8] In the spectrum for AK-2H, distinct peaks can be observed at 879 and 872 cm^{-1} for the CO_3 υ_2 modes for the A and B carbonate sites, respectively (Figure 1b). Additionally, peaks are observed between 1500 and 1300 cm^{-1} that agree well with those reported previously for the υ_3 modes of CO_3 in carbonated apatite. These same peaks are also apparent in the spectra of the AK-4 and AK-5H samples but are shifted to lower wavenumber with respect to those for AK-2H because of the ^{13}C enrichment. Although the CO_3 υ_2 region of the AK-4 sample does not contain a distinct doublet, an asymmetric peak is observed with its two components corresponding to the positions of the doublet. The presence of a doublet in the CO_3 υ_2 region in all spectra indicates that all samples are AB-type CHAp.[5,6,8] We also observe in the AK-2H sample CO_3 combination bands at 2520 and 2476 for $\upsilon_1 + \upsilon_3$ and at 2926 cm^{-1} for $2\upsilon_3$.[21] These same bands occur in the ^{13}C-enriched samples but are subsequently shifted toward lower wavenumbers.

Table 1. Comparison of Major IR and Raman Peak Positions in cm^{-1}; Raman Spectra Were Not Collected for the AK-2H Sample

	AK-2H	AK-2HD		AK-4		AK-5H		
assignment	IR	IR	Raman	IR	Raman	IR	Raman	ref
OH stretch	3571	3571		3572		3571		
H_2O	3376	3376		3329		3376		
$^{12}CO_3$ $2\nu_3$	2926	2926						
uncertain	2928							
$^{13}CO_3$ $2\nu_3$						2838		
OD stretch								
uncertain	2850							
$^{12}CO_3$ $\nu_1+\nu_3$	2520	2634	2636					
$^{13}CO_3$ $\nu_1+\nu_3$	2476			2464		2471		
						2434		
D_2O stretch		2495						
PO_4 $\nu_1+\nu_3$	2133	2138		2137		2135		
	2075	2075		2075		2075		
	1996	1998		1993		1997		
$^{12}CO_3$ ν_3	1466	1468						
	1418	1418						
$^{13}CO_3$ ν_3				1419		1414		
				1379		1376		
uncertain		1200						
PO_4 ν_3	1090	1091	1086	1093	1086	1092		4·14
CO_3 ν_1			1072		1072		1072	
PO_4 ν_3	1041	1043	1050	1040	1050	1044	1050	4·14
PO_4 ν_1	962	962	962	961	962	962	962	4·14
A $^{12}CO_3$ ν_2	879	879						5
B $^{12}CO_3$ ν_2	872	872		874		874		
A $^{13}CO_3$ ν_2				848		852		
B $^{13}CO_3$ ν_2						846		
PO_4 ν_4			608		608		608	
			590		590		590	
PO_4 ν_2			432		432		432	

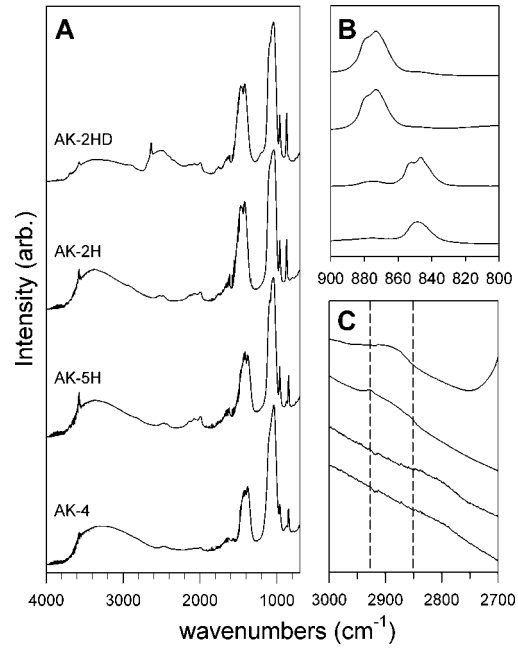

Figure 1. IR spectra of CAp samples from top to bottom: AK-2HD, AK-2H, AK-5H, and AK-4. (A) Full IR spectra from 4000 to 650 cm^{-1}. (B) Expanded view of CO_3 υ_2 region from 900 to 800 cm^{-1}. (C) Expanded view of the CO_3 $2\upsilon_3$ region from 2700 to 3000 cm^{-1}. Dashed lines correspond to the positions of the peaks at 2928 and 2850 cm^{-1} present in the spectrum taken of the sample AK-2H sample.

(17) Frydman, L.; Harwood, J. S. *J. Am. Chem. Soc.* **1995**, *117*, 5367.
(18) Amoureux, J. P.; Fernandez, C. *Solid State Nucl. Magn. Reson.* **1998**, *10*, 211.
(19) Wopenka, B.; Pasteris, J. D. *Mater. Sci. Eng., C* **2005**, *25*, 131.
(20) Joris, S. J.; Amberg, C. H. *J. Phys. Chem.* **1971**, *75*, 3172.

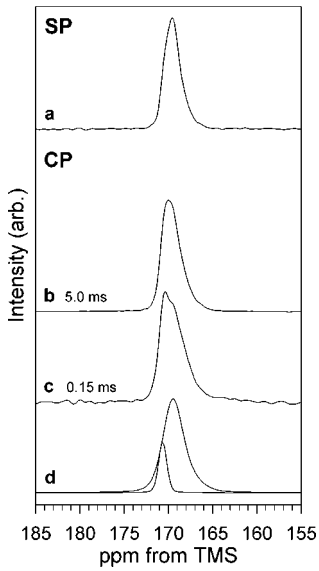

Figure 2. ^{13}C NMR spectra of CHAp sample AK-5H. (a) ^{13}C SP/MAS; 120 s relaxation delay, 32 acquisitions. (b) $^{13}C\{^1H\}$ CP/MAS; 5 ms contact time, 2 s relaxation delay, 4160 acquisitions. (c) $^{13}C\{^1H\}$ CP/MAS; 0.15 ms contact time, 2 s relaxation delay, 4160 acquisitions. (d) Spectral fit to c corresponding to peaks at 170.8 and an asymmetric peak at 169.8 ppm. All spectra were collected at a spinning rate of 3.0 kHz.

In response to NMR data that indicate the presence of weakly hydrogen bonded bicarbonate groups (see below), we deuterated the AK-2H sample (AK-2HD) but saw no significant shifting in the CO_3 regions. However, small peaks at 2928 and 2850 cm^{-1} that occur in the region that are usually assigned to CO_3 $2\upsilon_3$[21] can be observed to disappear with deuteration (Figure 1c). However, these peaks are also not apparent in spectra of the ^{13}C-enriched samples AK-4 and AK-5H. This result may indicate the presence of protonated carbonate in these samples; however, the vibrational spectra are inconclusive in this respect.

^{13}C NMR. The ^{13}C SP/MAS NMR spectrum of sample AK-5H shows a relatively broad, asymmetric peak (Figure 2a) centered near $\delta_C = 170$ ppm. This spectrum appears similar to that reported previously for a B-type carbonated apatite where an asymmetric peak at 170.2 ppm was observed.[7] The splitting of the CO_3 ν_2 peak in the FT-IR spectrum (see above), however, identifies this sample as AB-type CHAp. An additional peak at 166.5 ppm from A-type substitution is reported for AB-type CHAp[7] but is not observed in the present sample. Variable CP/MAS contact time experiments show systematic changes in peak shape that suggest the presence of at least two resonances in the peak at 170 ppm. At long contact times (Figure 2b), the peak exhibits a shape similar to that of the SP spectrum, but in spectra collected at short contact times, a second peak is clearly evident (Figure 2c). The variation in peak shape with contact time can be described by intensity changes of two components corresponding to a sharp peak at 170.8 ppm (1.3 ppm full width at half-maximum, fwhm) and a broader asymmetric resonance at 169.8 ppm (2.8 ppm fwhm; Figure 2d). The shape of the broad peak does not vary significantly with contact time and was represented, for purposes of spectral integration, by a sum of two Gaussian curves at constant intensity ratio. We also observe similar peak shapes in $^1H \rightarrow {}^{13}C\{^{31}P\}$ CP/REDOR spectra taken of the AK-5H sample (Figure SI-2, Supporting Information). Nearly identical lineshapes were observed in the control (S_0), REDOR (S), and REDOR difference spectra ($S_0 - S$), which indicate a close association of all the ^{13}C to ^{31}P. This result shows that all the ^{13}C species must be contained in the CHAp and that the distinct ^{13}C resonances cannot be distinguished easily on the basis of proximity to P. The ^{13}C chemical shift anisotropy (CSA) for spectra collected at contact times of 0.5 and 15 ms, obtained by fitting the integrated intensities of the spinning sidebands,[22] were very similar with spans (Ω) of 91.0 and 89.9 ppm and skews (κ) of 0.42 and 0.51, respectively.

The CP dynamics were analyzed by fitting variable contact time $^{13}C\{^1H\}$ CP/MAS spectra to the same components (Figure 2d), allowing only the intensities to vary. The experimental conditions, unmodulated continuous wave (CW) polarization transfer, and a spinning rate of 3.0 kHz, were chosen to allow direct comparison with a previous study of carbonate groups.[23] These results indicate that two separate ^1H spin reservoirs contribute intensity to each of the ^{13}C resonances represented by the peaks at 169.8 and 170.8 ppm. Each ^{13}C peak exhibits biexponential CP intensity buildup with a small apparent fraction (13−34%) of the intensity increasing quickly with contact time (T_{CH} values of 0.8 and 0.7 ms) and the remainder exhibits a slower rate defined by T_{CH} values of 4.7 and 6.6 ms for the peaks at 169.8 and 170.8 ppm, respectively (Figure SI-3, Supporting Information). These data did not allow the $T_{1\rho,H}$ values to be determined because the intensities continued to increase for all contact times. We independently measured the ^1H $T_{1\rho}$ by introducing a delay before the contact pulse to allow the ^1H to evolve under the spin locking pulse. At constant contact time, the $^{13}C\{^1H\}$ CP/MAS intensity decays according to a biexponential function (Figure SI-4, Supporting Information). This result indicates the presence of at least two proton spin reservoirs associated with the ^{13}C with a subset of spins characterized by a short $T_{1\rho,H}$ of 1.8 ms (32%), whereas the majority relax more slowly with a value of $T_{1\rho,H} = 33$ ms.

HetCor NMR. $^{13}C\{^1H\}$ two-dimensional HetCor NMR spectra were acquired for the AK-5H sample at a variety of contact times to examine the relationship between the H and carbonate groups in this system. A typical spectrum is shown in Figure 3 as a contour plot. The summed ^1H projections contain three peaks, centered near $\delta_H = 0.0$, 1.3, and 5.5 ppm, the latter of which is broad and asymmetrical with a tail extending to 11 ppm. The peaks at 1.3 and 5.5 ppm are prominent in the ^1H summed projections collected at short contact time, whereas the peak centered about 0.0 ppm grows to become the dominant peak in the spectra at long contact times (Figure 4a). The contour plot also shows clearly the presence of two ^{13}C resonances at $\delta_C = 170.8$ and 169.8 ppm, which were inferred from the CP/MAS spectra at variable contact time. The summed ^{13}C projections (Figure

(21) Genge, M. J.; Jones, A. P.; Price, G. D. *Geochim. Cosmochim. Acta* **1995**, *59*, 927.
(22) Herzfeld, J.; Berger, A. E. *J. Chem. Phys.* **1980**, *73*, 6021.
(23) Feng, J.; Lee, Y.; Reeder, R. J.; Phillips, B. L. *Am. Mineral.* **2006**, *91*, 957.

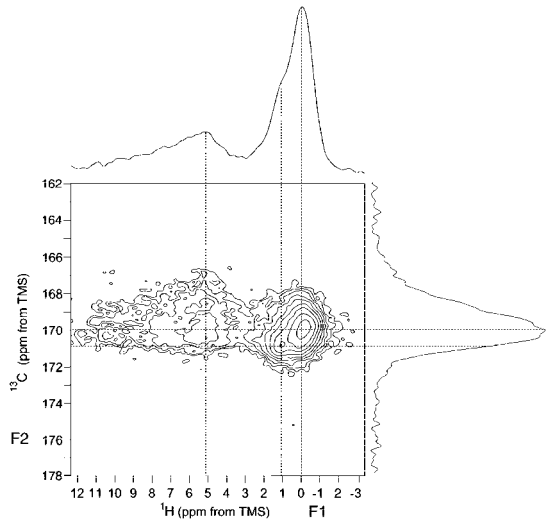

Figure 3. Two-dimensional ^{13}C{^{1}H} HetCor spectrum of AK-5H collected at a contact time of 3 ms and a spinning rate of 10 kHz. Spectra at top and side are summed projections over the centerband intensity.

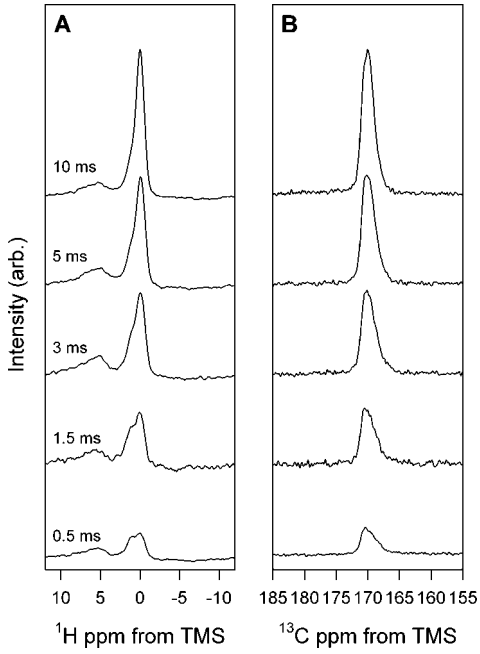

Figure 4. Projections of ^{13}C{^{1}H} HetCor NMR spectra of sample AK-5H collected at the indicated contact times. (A) Indirectly detected ^{1}H spectra summed over the ^{13}C centerband. (B) ^{13}C spectra summed over the ^{1}H dimension. Spectra are scaled to reflect absolute intensity per scan.

4b) show similar changes in peak shape with increase of contact time as those collected for the variable contact time ^{13}C{^{1}H}CP/MAS experiment (Figure 2).

The HetCor spectra indicate that the resolved carbonate environments are distinguished by association with different ^{1}H environments and that the H environments are strongly related to carbonate substitution. The peak at $\delta_C = 170.8$ ppm displays a correlation with the $\delta_1H = 5.5$ peak that appears weak because of the width of this peak, whereas apparent stronger correlations for this site are observed with the proton resonances at $\delta_H = 0.1$ and 1.3 ppm because of their narrow lineshapes (Figure 5a). At short contact times, the carbonate resonance at $\delta_C = 169.8$ ppm is most strongly

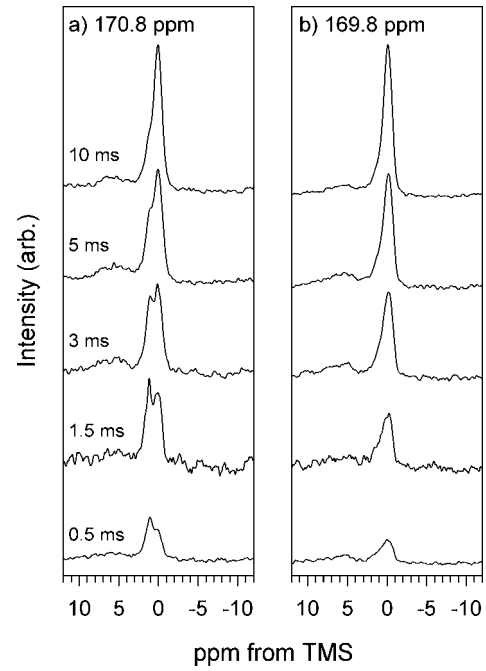

Figure 5. ^{1}H Traces (F1) from two-dimensional ^{13}C{^{1}H} HetCor spectra of AK-5H taken at the indicated contact times, corresponding to the F1 cross sections at the main ^{13}C peak positions in F2 at (a) $\delta_C = 170.8$ and (b) 169.8. Spectra are scaled to reflect absolute intensity per scan.

correlated to peaks at $\delta_H = -0.1$ and 5.5 ppm (Figure 5b). The CP dynamics for each ^{1}H/^{13}C cross-peak were determined by fitting the ^{1}H slices (F1) taken at the respective ^{13}C isotropic chemical shift to a sum of Gaussian curves. The fitted relative intensities were scaled to total integrated intensities obtained from ^{13}C{^{1}H} CP/MAS variable contact time spectra acquired under the same conditions (Figure 6). Corresponding T_{CH} and $T_{1\rho,H}$ values (Table 2) were determined by fitting the intensities to a classical CP dynamics curve.[24] The ^{1}H(5.5)/^{13}C(169.8) cross-peak exhibits a quick intensity buildup characterized by a T_{CH} value of 0.8 ms and decay with an apparent $T_{1\rho,H}$ value of 12 ms. The peaks at 1.3 and -0.1 ppm exhibit slower intensity buildups with T_{CH} values of 2.7 and 4.3 ms, respectively. This result indicates that the ^{1}H species represented by the peak at 5.5 ppm are more closely associated with this carbonate site than those at 1.3 and -0.1 ppm. The CP dynamics for the carbonate site at $\delta_C = 170.8$ ppm are characterized by T_{CH} values of 0.8, 0.7, and 3.6 ms for the sites at $\delta_1H = 5.5$, 1.3, and 0.1 ppm, respectively. This result suggests strong coupling between this carbonate site to the peaks at 5.5 and 1.3 ppm and a weak correlation to that at 0.1 ppm. Although the ^{1}H peak at 5.5 ppm does not appear prominent in the spectra, its intensity is significant at short contact times because of its large width. However, comparison of the contour plot (Figure 3) and fitted ^{13}C spectral components (Figure 2d) suggests it is likely that much of the apparent ^{1}H(5.5)/^{13}C(170.8) cross-peak intensity corresponds to overlap with the ^{13}C peak at 169.8 ppm.

Additional ^{13}C{^{1}H} HetCor spectra were collected at a contact time of 10 ms with a mixing time introduced between

(24) Kolodziejski, W.; Klinowski, J. *Chem. Rev.* **2002**, *102*, 613.

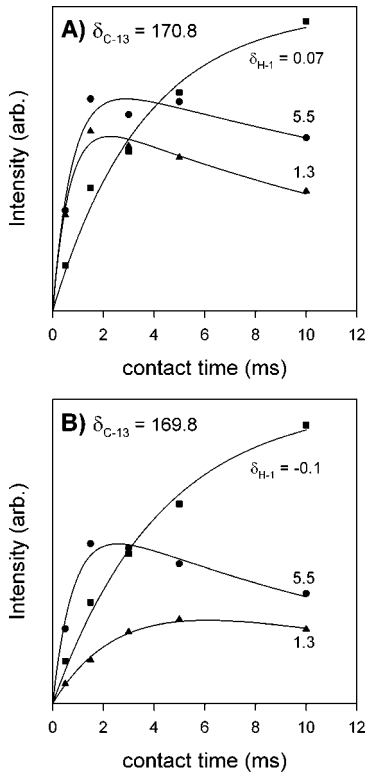

Figure 6. Variation in the cross-peak intensity of the $^{13}C\{^1H\}$HetCor NMR spectra taken of sample AK-5H for ^1H slices taken at (A) 170.8 ppm and (B) 169.8 ppm. Symbols represent the integrated intensity for the ^1H sites at 0.1 and −0.1 ppm (■), 1.3 ppm (▲), and 5.5 ppm (●). Lines represent a least-squares fit to classical CP dynamics.[24]

Table 2. CP Kinetic Values Obtained for the ^1H HetCor Cross-Peaks

δ_C	δ_H	I_0	T_{CH} (ms)	$T_{1\rho,H}$[a] (ms)
169.8	−0.1	0.48(1)	4.3(1)	>100[b]
	1.3	0.22(3)	2.7(3)	18(2)
	5.5	0.30(2)	0.8(2)	17(1)
170.8	0.1	0.53(1)	4.3(1)	>100[b]
	1.3	0.24(1)	0.7(1)	18(1)
	5.5	0.23(3)	0.8(3)	12(2)

[a] $T_{1\rho,H}$ values reported are apparent values. [b] Value fixed to obtain suitable fit. See text.

^1H excitation and the $^1H \rightarrow {}^{13}C$ polarization transfer.[25] This experiment indicates whether the short apparent ^1H $T_{1\rho}$ values observed for the various ^1H sites by HetCor contain a contribution from $^1H-{}^1H$ spin diffusion to an abundant ^1H reservoir at long contact times. We observe that as the mixing time increases from 20 to 40 ms, the cross-peaks at δ_H = 1.3 and those near 0.0 ppm remain at a constant intensity, whereas that at 5.5 ppm gradually decays at a rate consistent with the apparent value of $T_{1\rho,H}$ = 12 ms measured for this peak. This result indicates that the short apparent $T_{1\rho,H}$ for the peak at 5.5 ppm results from spin diffusion to a bulk ^1H reservoir. However, the peak at 1.3 ppm appears to represent a distinct ^1H reservoir that relaxes to thermal equilibrium before spin diffusion to the other peaks, giving a distinct $T_{1\rho,H}$. These results are consistent with the $^{13}C\{^1H\}$ CP/MAS

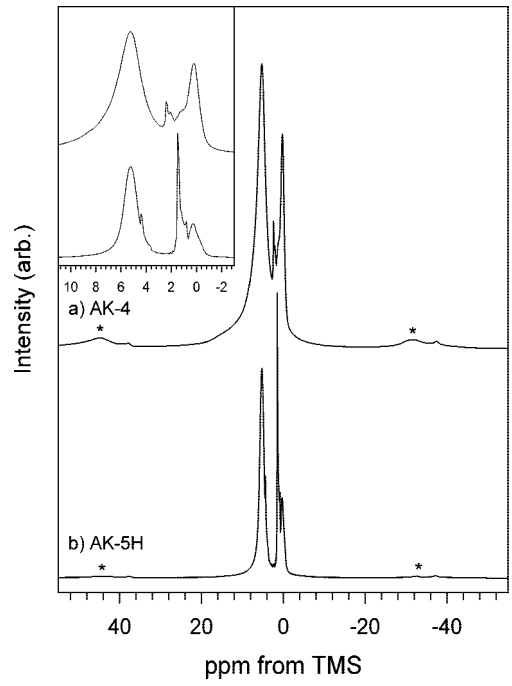

Figure 7. ^1H SP/MAS NMR spectra of CHAp samples (a) AK-4 and (b) AK-5H. Inset: Expanded view of the centerband region of each spectrum. Each spectrum was collected with a 1 s relaxation delay at a spinning rate of 15 kHz for 128 and 512 acquisitions, respectively. Asterisks denote spinning sidebands.

$T_{1\rho,H}$ measurements (Figure SI-4, Supporting Information), although absolute values from HetCor are larger, probably because of the faster spinning rate.

$^{31}P\{^1H\}$ HetCor NMR spectra were also taken of the AK-5H sample to examine whether the proton environments observed in the $^{13}C\{^1H\}$ HetCor NMR spectra also occur near phosphate in the apatite (Figure SI-5, Supporting Information). The ^{31}P projection shows a single peak at δ_P = 2.8 ppm (1.3 ppm fwhm). The ^1H projection exhibits peaks at δ_H = 0.2, 1.3, and 5.5 ppm, similar to those observed in the $^{13}C\{^1H\}$ HetCor NMR spectra. In this case, however, the peaks at 1.3 and 5.5 ppm are much weaker and that at 1.3 ppm appears not as a distinct peak but rather as a weak shoulder on the dominant 0.2 ppm peak. The ^1H peak at 5.5 ppm is somewhat sharper than that in the $^{13}C\{^1H\}$ HetCor, suggesting that the $^1H(5.5)/^{31}P(2.8)$ cross peak might correspond to different environments such as HPO_4 groups or H_2O molecules, which can give similar shifts,[26,27] but the data are inconclusive. These results indicate an association of the ^1H peaks at 1.3 and 5.5 ppm with phosphate and show that these hydrogrens occur in the apatite structure.

^1H MAS NMR. The ^1H SP/MAS NMR spectra show a complex set of peaks for the ^{13}C-enriched CHAp samples (Figure 7). These spectra are dominated by three peaks at chemical shifts of δ_H = 0.2, 1.3, and 5.2 ppm. An additional set of sharp peaks occur in the spectrum for AK-4 near 2.3 ppm that contribute less than 2% of the total intensity and do not occur in HetCor spectra taken of this sample (not shown); they are assigned to unknown impurities or surface

(25) Schmidt-Rohr, K.; Clauss, J.; Spiess, H. W. *Macromolecules* **1992**, *25*, 3273.
(26) Cho, G.; Wu, Y.; Akerman, J. L. *Science* **2003**, *300*, 1123.
(27) Jager, C.; Welzel, T.; Meyer-Zaika, W.; Epple, M. *Magn. Reson. Chem.* **2006**, *44*, 573.

sites. A broad component centered at about 11.6 ppm occurs in this spectrum that is similar to that assigned to HPO_4 groups in nanocrystalline hydroxylapatite[26] but its identity in this sample is uncertain.

Comparison of the spectra for AK-4 and AK-5H show that the hydrothermal treatment affects the proton environments present in the samples, although drying methods also could account for some differences. The spectrum of the AK-5H exhibits decreased linewidths in comparison to that for AK-4 with the major peak at 5.2 ppm decreasing from a linewidth of 1.8 ppm to a fwhm of 1.1 ppm. The set of peaks near 2.3 ppm and the broad peak at 11.6 ppm are not present in the spectrum of the AK-5H sample. There is, however, an additional sharp peak at 4.8 ppm (0.1 ppm fwhm), which given its position and narrow line width likely arise from fluid water, either as inclusions or adsorbed on the surface. Although the chemical shift region of 2 to −1 ppm in the spectrum of AK-5H contains several overlapping peaks, the HetCor data (described above) contain only the resonances at 1.3 ppm and near 0 ppm. Comparison of the ^{1}H spectra obtained from the ^{13}C and ^{31}P HetCor data with these direct-observe spectra shows that the CHAp contains many H environments that are not directly associated with the apatite structure or are mobile on the NMR time scale, but are likely to contribute to the OH stretch region of the vibrational spectra.

^{23}Na NMR. Because replacement of Ca^{2+} in the structure by Na^+ has been proposed as a method for charge balancing carbonate substitutions in CHAp[5,9] and chemical analysis showed significant Na content, we studied the AK-5H sample with ^{23}Na NMR techniques. The ^{23}Na SP/MAS spectra at both 9.4 and 11.7 T show a broad, asymmetric peak (Figure 8a). ^{23}Na{^{31}P} REDOR spectra were taken over a variety of dephasing periods to investigate the connectivity between Na and P. Although this technique can be used as a method for determining P−Na distances,[28] in this instance, we used it only as a spectral editing technique. We observed similar peak shapes for the ^{23}Na control spectrum (S_0; Figure 8b), the ^{23}Na{^{31}P} REDOR spectrum (S; Figure 8c) and the REDOR difference spectrum ($S_0 - S$; Figure 8d). The REDOR fraction ($1 - S/S_0$) under these conditions reaches unity at 4 ms dephasing time, indicating that all of the Na in the sample is associated with P and therefore contained in the CHAp and not a separate phase. Comparison of the ^{23}Na SP (Figure 8a) and ^{23}Na spin–echo spectra (S_0, Figure 8b) shows the presence of a narrow component in the former that does not appear in the spin–echo data, probably because of a short T_2. However, ^{23}Na MQMAS spectra (Figure SI-6, Supporting Information) do not resolve distinct ^{23}Na resonances and instead show two-dimensional peak shapes consistent with distributions in both chemical shift and quadrupolar coupling. This result indicates that the Na is disordered in the CHAp with a distribution of orientations and bond distances. The SP data at both 11.7 and 9.4 T can be fit with a sum of quadrupolar MAS lineshapes corresponding to a distribution of electric field gradients[29] that approximates a Gaussian distribution of quadrupolar coupling constants with an average of 1.2 MHz and a width of 2.6 MHz (fwhm, truncated at $C_Q = 0$) at an average isotropic chemical shift of $\delta_{Na} = -3.9$ ppm.

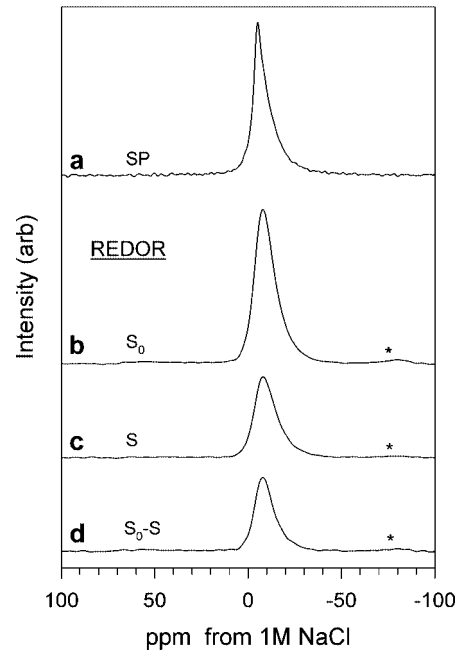

Figure 8. ^{23}Na MAS NMR spectra of sample AK-5H (a) SP MAS NMR spectrum collected at a spinning rate of 18 kHz and pulse delay of 0.5 s. (b−d) ^{23}Na{^{31}P} REDOR collected with a 1.4 ms dephasing period, 10 kHz spinning rate, and 0.5 s pulse delay: (b) ^{23}Na spin–echo control, S_0; (c) ^{23}Na{^{31}P} REDOR, S; (d) difference spectrum, $S_0 - S$. Spectra are scaled to reflect the absolute intensities. Asterisks denote spinning sidebands.

Discussion

^{1}H Peak Assignments of carbonate-associated H. Our results from the ^{1}H SP/MAS and HetCor spectra indicate that the carbonate groups are associated with several distinct H species. Although the position of the peak at 0.2 ppm observed in the ^{1}H SP/MAS and the ^{31}P{^{1}H} HetCor is in good agreement with those previously observed by ^{1}H SP/MAS for hydroxyl groups in hydroxylapatite,[15] close examination of the ^{13}C{^{1}H} HetCor data show that the hydroxyl resonance is slightly shifted to 0.1 and −0.1 ppm in slices taken at $\delta_C = 170.8$ and 169.8 ppm, respectively. The intensity of these peaks increases slowly with contact time in all the ^{13}C{^{1}H} HetCor slices, indicating that this proton environment is well-removed from the carbonate carbon. The long T_{CH} values (3−4 ms) are consistent with long H−C distances and comparable to the T_{PH} values observed for pure HAp.[27] Considering that, for HAp, a ^{1}H chemical shift of 0.2 ppm corresponds to a $d(O\cdots O) = 3.44$ Å,[30] these peaks at 0.1 and −0.1 ppm suggest somewhat longer O···O distances near the carbonate substitution.[31] We therefore assign these peaks to hydroxyl groups at positions that are perturbed slightly from the normal hydroxyl position by the insertion of carbonate.

(28) Strojek, W.; Eckert, H. *Phys. Chem. Chem. Phys.* **2006**, *8*, 2276.
(29) Coster, D.; Blumenfeld, A. L.; Fripiat, J. J. *J. Phys. Chem.* **1994**, *98*, 6201.
(30) Sanger, A. T.; Kuhs, W. F. *Z. Kristallogr.* **1992**, *199*, 123.
(31) Yesinowski, J. P.; Eckert, H.; Rossman, G. R. *J. Am. Chem. Soc.* **1988**, *110*, 1367.

The cross-peak at $\delta_H = 1.3$ ppm exhibits a very rapid intensity buildup in the HetCor slices taken at $\delta_C = 170.8$ ppm, corresponding to a T_{CH} value (0.7 ms) that is similar to the initial $^1H \rightarrow {}^{13}C$ polarization transfer for bicarbonate defects in calcite.[23] Such short T_{CH} requires C−H distances (ca. 2 Å) that are too short to be accounted for by hydroxyl groups hydrogen-bonded to carbonate, especially considering that this ^1H chemical shift indicates a weak H-bonding environment (d(O···O) ≈ 3.0 Å).[31] For comparison, chemical shifts reported for strongly hydrogen-bonded bicarbonate are much higher for phases such as nahcolite ($NaHCO_3$; $\delta_H = 14.1$ ppm) and trona ($Na_3H(CO_3)_2(H_2O)_2$; $\delta_H = 18.6$ ppm), which have a d(O···O) of 2.55 and 2.37 Å, respectively.[23] Therefore, we interpret the combination of short T_{CH} values and small ^1H chemical shift to indicate H directly bonded to carbonate ion that is a weak hydrogen-bond donor. These results indicate significant contribution of bicarbonate to the peak at 170.8 ppm such that it accounts for about 24% of the polarization transfer from CP kinetics (Table 2).

Previous studies have noted distinct differences of ^{13}C chemical shift and CSA between alkali bicarbonates and their carbonate-containing counterparts[32] (e.g, $KHCO_3$: $\delta_C = 159.9$ ppm, $\Omega = 97$ ppm, $\kappa = -0.46$; K_2CO_3: $\delta_C = 169.3$ ppm, $\Omega = 82$ ppm, $\kappa = 0.61$). In these compounds, bicarbonate groups accept and donate strong hydrogen bonds. In contrast, bicarbonate defects in calcite, which are moderate hydrogen bond donors ($\delta_H = 7.4$ ppm), exhibit ^{13}C chemical shift and CSA that are nearly indistinguishable from those of the bulk carbonate groups (HCO_3: $\delta_C = 168.7$ ppm, $\Omega = 84$ ppm, $\kappa = 0.55$: CO_3: $\delta_C = 168.7$ ppm, $\Omega = 76$ ppm, $\kappa = 0.95$).[23] The CSA patterns in $^{13}C\{^1H\}$ CP/MAS NMR spectra of CHAp at short contact time ($\Omega = 91.0$ ppm, $\kappa = 0.43$) match well those observed for bicarbonate defects in calcite.[23] Therefore, it appears that ^{13}C chemical shift parameters are insufficient to identify the difference between carbonate and bicarbonate in weakly hydrogen bonded systems.

The peak at 1.3 ppm also appears to contribute about 22% of the intensity to the ^{13}C cross-peak at 169.8 ppm (Table 2). However, this peak is not well-resolved in the ^1H slices taken at 169.8 ppm and its intensity was obtained from fits in which the peak width and position were fixed to those derived for the $^1H(1.3)/^{13}C(170.8)$ cross-peak. Although it is possible that the intensity of this peak in the ^1H slices at 169.8 ppm is just the tail of the peak at 0.1 ppm, the much different $T_{1\rho,H}$ values indicates distinct H species. Although the $^1H(1.3)/^{13}C(169.8)$ cross-peak exhibits a longer T_{CH} value than that of the $^1H(1.3)/^{13}C(170.8)$ cross-peak (2.7 and 0.7 ms, respectively) the $T_{1\rho,H}$ values (18 ms) are the same within uncertainty, suggesting that these cross-peaks correspond to the same H environment that is associated with both types of carbonate, but further removed from the carbonate at $\delta^{13}C = 169.8$ and closer to that at 170.8 ppm.

The peak at $\delta_H = 5.5$ ppm exhibits a quick buildup of CP intensity in both the HetCor slices taken at $\delta_C = 170.8$ and 169.8 ppm. However, the resolution in the ^{13}C dimension is poor and the contour plots suggest that these H environments are associated primarily with the peak at 169.8 ppm. This assignment is consistent with the considerable overlap of the peaks at 170.8 and 169.8 ppm (Figure 2d), the larger width of the latter, and the very similar CP kinetics fit to the 170.8 and 169.8 ppm slices. The $^1H(5.5)/^{13}C(169.8)$ cross-peak also exhibits a short T_{CH} similar to that observed for bicarbonate defects in calcite,[23] indicative of a short C−H distance. Although the ^1H chemical shift of this cross-peak corresponds well to that observed for water contained in apatite[26,27] assignment of the short observed T_{CH} value to carbonate−water interaction would require a very short hydrogen bond distance and consequently a much more positive ^1H chemical shift value. We also observe that this peak decays when a mixing time is introduced in the HetCor experiment, indicating that spin diffusion to the main ^1H reservoir near 0 ppm accounts for the short apparent $T_{1\rho,H}$. We therefore assign the $^1H(5.5)/^{13}C(169.8)$ cross-peak to A-type bicarbonate groups in the channel sites that donate moderate hydrogen bonds, possibly to adjacent hydroxyl in the channels. The broad asymmetric line shape in the ^1H-dimension with intensity tailing out to about 11 ppm corresponds to a wide range of hydrogen bond lengths with d(O···O) values ranging from about 2.88 to 2.66 Å.[31] On this basis, the corresponding OH stretch in FT-IR spectra can be expected to give a broad, ill-defined peak spanning 2982 to 3399 cm^{-1} [33] that could be difficult to observe.

A-Type Substitution. On the basis of the assignments made from our NMR data, approximately 28% of the total carbonate present is represented by bicarbonate groups (Table 2). The presence of bicarbonate groups also implies additional defect structures to those suggested previously in CHAp. In the case of A-type (channel) carbonate, the commonly reported method for substitution is the removal of two hydroxyl groups for the inclusion of a single carbonate group.[8,11]

$$[{}^{A}CO_3^{2-} = 2OH^-]$$

Peroos et al.[34] studied this substitution method in CHAp using molecular dynamics simulations and found that the most stable configuration of this A-type carbonate defect occurred with the carbonate ion located midway between the two hydroxyl positions. The calculated minimum-energy configuration for this defect leads to a long hydrogen bond interaction between the carbonate oxygens and the channel hydroxyl with a d(O···O) distance of 2.75 Å. This distance corresponds well to the d(O···O) distance range of 2.66 to 2.88 Å derived for the bicarbonate group represented by the broad peak at $\delta_H = 5.5$ ppm. The charge imbalance from protonation of the carbonate could be compensated through the coupling of the A-type substitution with a corresponding Na^+ defect

$$[Na^+ + {}^{A}HCO_3^- = Ca^{2+} + 2OH^-]$$

The large molar Na/carbonate ratio found for our samples supports such a coupled substitution. One possible advantage of bicarbonate groups is that this configuration would allow the hydroxyl ordering within the channels to be preserved

(32) Stueber, D.; Orendt, A. M.; Facelli, J. C.; Parry, R. W.; Grant, D. M. *Solid State Nucl. Magn. Reson.* **2002**, *22*, 29.
(33) Libowitzky, E. *Monatsh. Chem.* **1999**, *130*, 1047.
(34) Peroos, S.; Du, Z. M.; de Leeuw, N. H. *Biomaterials* **2006**, *27*, 2150.

without significant perturbations of the hydroxyl ions in the channel sites. Weak interaction of a nonprotonated carbonate oxygen with a hydroxyl could explain the cross peak at $\delta_H = 1.3$ ppm in CHAp, which corresponds well to that observed for a hydroxyl group in fluorhydroxylapatites.[15] However, this chemical shift would correspond to an O···O distance longer than the 2.75 Å from the computation models.

AB-Type Substitution. Previous studies have suggested that a coupled substitution is not only possible but in cases required for the incorporation of carbonate into both the A and B site in type AB CHAp.[9,34] Computational models[34] suggest that a substitution for the AB-type defect can be accommodated by the removal of a channel hydroxyl and the movement of a channel hydroxyl to a position next to the B-type carbonate group.

$$[2CO_3^{2-} = PO_4^{3-} + {}^{A}OH^{-}]$$

It was found that this configuration gives the most energetically favorable defect of all A, B and AB-type substitution methods studied. However, this arrangement requires not only a proximity of the B-hydroxyl to the carbonate group (d(O···O) = 2.24−2.77 Å), but also a crowding of the A-type carbonate because of the substitution for one channel hydroxyl instead of two. We find no evidence for a hydroxyl with such short hydrogen bond lengths; all H with large chemical shifts appear to correspond to bicarbonate groups. Astala and Stott[35] suggest that the B-type carbonate is best accommodated through a Ca vacancy and a corresponding HPO_4 substitution. In this study, a C−H distance of 3.79 Å was reported for the lowest energy configuration for this defect, which suggests a d(O···O) > 4 Å for the corresponding hydrogen bond assuming a typical geometry. A small amount of such weakly hydrogen bonded HPO_4 would be difficult to detect by the methods used in the present study because it would likely overlap the ^{1}H hydroxyl resonances. Fleet and Liu[9] suggest that a coupled AB-type substitution could be accomplished through an additional substitution of a Na^+ for Ca^{2+}, but they do not propose a specific charge balance mechanism. On the basis of this information, we can propose an additional substitution that incorporates bicarbonate into the B-site through a coupling with an A-site substitution and Na

$$[Na^+ + {}^{B}HCO_3^- + {}^{A}CO_3^{2-} = Ca^{2+} + PO_4^{3-} + OH^-]$$

This substitution method would eliminate the need for an additional hydroxyl group to be incorporated with the B-type substitution. The replacement of two hydroxyl groups in the channels for one carbonate group would allow for less steric hindrance of the A-type substitution but would require a second Na^+ for charge balance. If the orientation of the bicarbonate ion in the channel is similar to that proposed by Fleet and Liu,[9] lying more or less parallel to one of the far faces of the phosphate ion, the smallest d(O···O) distance for the bicarbonate ion to the closest oxygen of the nonprotonated carbonate group would be about 3.05 Å. This geometry is in good agreement with the d(O···O) value 3.04 Å estimated from the chemical shift of the ^{1}H cross-peak at 1.3 ppm. Observation of similar $T_{1\rho,H}$ values (18 ms) for both the ^{1}H(1.3)/^{13}C(170.8) and the ^{1}H(1.3)/^{13}C(169.8) cross-peaks is consistent with a contribution from a single H environment associated with both carbonate environments as expected for such a coupled substitution. In this case, the short T_{CH} of the ^{1}H(1.3)/^{13}C(170.8) cross-peak indicates protonation of the B-type carbonate.

Acknowledgment. We thank three anonymous reviewers for the insightful comments that led to many improvements to the manuscript. This work was supported by the Center for Environmental Molecular Science, which is funded by the NSF EMSI program (CHE-0221934) and NSF CHE-03-21001, for instrumentation.

Supporting Information Available: Additional figures, including Raman spectra, ^{1}H → ^{13}C{^{31}P} REDOR spectra, plots of ^{13}C{^{1}H} CP/MAS kinetics, ^{31}P{^{1}H} HetCor contour plot, and ^{23}Na MQMAS contour plot (PDF). This information is available free of charge via the Internet at http://pubs.acs.org.

CM0716598

(35) Astala, R.; Stott, M. J. *Chem. Mater.* **2005**, *17*, 4125.